

Evolution of Fat Crystal Network Microstructure Followed by NMR

Matthieu Adam-Berret,^{†,‡,§} Marine Boulard,^{†,§} Alain Riaublanc,[‡] and François Mariette^{*,†,§}

[†]Cemagref, UR TERE, 17 Avenue de Cucillé, CS 64427, F-35044 Rennes, France

[‡]INRA-BIA, Rue de la Géraudière, BP 71627, 44316 Nantes cedex 3, France

[§]Université européenne de Bretagne, France

ABSTRACT: Model systems composed of tristearin in solid state and tricaprins in liquid state with different solid-fat content (SFC) and storage time have been investigated by relaxation NMR and NMR diffusometry. The T_2 relaxation of the tricaprins in the melt exhibited a bimodal distribution as previously observed. The SFC had a major effect on the T_2 relaxation. This effect was explained according to the fast diffusive exchange model in porous media. According to this model the changes in T_2 relaxation as a function of the SFC and storage time were explained by the decrease of the surface-to-volume ratio of the crystal induced by Ostwald ripening. The diffusion coefficient D of the tricaprins in the melt decreased for higher SFC. Since no significant variation of D was observed for different diffusion time, D reflected the long-range connectivity and the tortuosity was calculated. During storage the diffusion coefficient remained constant.

KEYWORDS: low-field NMR, relaxation, diffusion, triacylglycerols, specific surface, tortuosity

INTRODUCTION

Triacylglycerols are very present in our food because they are the main constituents of fat-containing products such as butter and chocolate. The characteristics of the fat crystal network created by triacylglycerols contribute to many of the physical properties of food products, but also of pharmaceutical and cosmetic compounds.^{1,2} It is thus of paramount importance for the industry to monitor the properties of the fat crystal network, which is known to evolve during storage. This instability of the network leads to undesired modifications of the functional properties of foods such as texture, morphology and taste. Thus, knowledge of the physical properties is critically important for improving the functionality of end products under processing and storage. However, it is not so easy to monitor the behavior of fats because different levels of organization have to be considered for the solid phase and because the behavior of the liquid phase is still poorly understood. At least three levels of organization have been proposed for the solid phase, i.e. polymorphism on the angstrom scale, crystal size on the micrometer scale and flocs on the millimeter scale. Moreover, these parameters depend on the method of crystallization and evolve over time. Indeed, there are three main polymorphic forms for triacylglycerols: the α (hexagonal subcell), β' (orthorhombic perpendicular subcell) and β (triclinic parallel subcell) forms, the latter being the most stable; and thus triacylglycerols crystallized in the α and β' forms tend to evolve to the β form.³ Moreover, fat crystals continue to grow upon crystallization because of the Ostwald ripening phenomenon.⁴ The network can thus evolve for months before reaching an equilibrium state.⁵ The liquid phase behavior is equally not without significance. Two models are presently used to describe the liquid phase, namely, the smectic model and the nematic model. The former, proposed by Larsson⁶ and maintained by Sato et al.,⁷ assumes that melted triacylglycerols are in a para-lamellar arrangement which provides long-term order in

X-ray diffraction 20–40 °C above the melting point. Conversely, Cebula et al.⁸ suggested that there was no organization in the liquid state and that triacylglycerols exist in disorder. Corkery et al.⁹ recently proposed an intermediate between the smectic and nematic models for triacylglycerols with a discotic model which may explain the differences between Larsson and Cebula. This model was strengthened by a study using Raman spectroscopy.¹⁰ Finally, fats in natural resources are mixtures of different types of triacylglycerols, which complicates the melting behavior, crystallization, crystal morphology and aggregation in real fat systems.¹¹

As rheological, textural and functional properties of food are related to the microstructure of the fat crystal network,¹² many attempts have been made to suggest a model for the network. A mechanical model was originally developed by van den Temple¹³ in which van der Waals attraction held aggregated fat particles. However, the network properties cannot be described quantitatively with this model. Introduction of the fractal dimension for colloidal gels early in the 1990s opened up new prospects for the characterization of fats. Vreeker et al. was the first to suggest that fat crystal networks should be considered as a fractal structure.¹⁴ They used the fractal dimension to quantify the relationship between the mass of a cluster and its size. Later, Marangoni et al. developed the applications of the fractal model in two and then three dimensions. They related the elastic modulus of colloidal networks, especially fat crystal networks, to the volume fraction of solids. They proposed a model in which fats are composed of many parallel straight fat crystal cluster chains in a whole homogeneous, space-filling and perfectly connected network.¹⁵

Received: July 15, 2010

Accepted: December 28, 2010

Revised: December 20, 2010

Published: February 11, 2011

Liang et al. confirmed this model and depicted the fat as a porous interconnected medium filled with liquid oil.¹⁶ The fractal dimension is currently determined by rheological measurements and polarized light microscopy. However, there is a real need for understanding of the microstructure of the fat crystal network.

NMR has already been used for the study of triacylglycerols. However, most of the results published have concerned the solid phase. NMR has proved to be effective for the determination and quantification of polymorphism,^{17–20} and different studies have reported on the mobility of the triacylglycerol side chains in the solid state.^{21,22} A recent study proved the capacity of spin–lattice relaxation time measurements of the solid phase to obtain information about crystal size.⁴ In the opposite, the liquid phase was less investigated by NMR. Spin–spin relaxation measurements of the liquid phase have highlighted a biexponential behavior for the liquid phase of milk and vegetable fat.²³ As the structural organization of the liquid phase remains unknown, it is difficult to explain this behavior. However, the phenomenon may be explained by more rapid movement of the methyl group at the end of the chain, as observed for stearic acid diluted in a solvent.²⁴

In recent years, nuclear magnetic resonance (NMR) techniques have been used for the study of porous media due to their nondestructive and noninvasive properties. Although the behavior of confined liquid molecules at the pore wall interface has only partially been characterized, this technique has been used extensively in the study of microstructurally complex materials such as rock, cements, biological cells, pharmaceutical compounds and emulsions.^{25–27} The surface-to-volume ratio, characteristic of the microstructure, the pore size distribution and the tortuosity can be measured by NMR through either signal relaxation or pulsed field gradient (PFG) NMR measurement techniques.^{28,29} The only application of PFG-NMR for fats is the determination of droplet size distribution in O/W emulsions. The principle is based on the restricted diffusion (as for porous media) of the molecules inside droplets.³⁰

The aim of this study was to evaluate the sensitivity of the NMR relaxation and diffusion parameters from the liquid fat phase to the microstructure of the fat crystal network and to the solid fat content. Based on the properties of restricted diffusion and surface relaxation, NMR relaxation and diffusion measurements for the liquid phase were investigated in order to evaluate the potentials of this technique for the characterization of the fat crystal network.

EXPERIMENTAL PROCEDURES

Materials and Tempering Procedures. Tricaprin and tristearin were purchased commercially (Sigma, St. Louis, MO, USA; >98% purity) and samples were used without any further purification.

To study the microstructure, tricaprin and tristearin were blended in the melted state at ratios of 25/75, 40/60, 50/50, 60/40, 67/33 and 75/25 (w/w). The mixtures were melted at 80 °C for 20 min and then crystallized at 5 °C for 10 min in a cryocooler. Each sample was inserted inside the spectrometer heated to 60 °C. At the latter temperatures, tricaprin was in the liquid state and tristearin in the solid state. The temperature of the sample was maintained at 60 °C in an oven or in the spectrometer to avoid the recrystallization of the liquid phase, and measurements were done on this liquid phase.

NMR Experimental Protocol. NMR measurements were carried out with a 0.47 T NMR spectrometer (Minispec MQ20, Bruker SA, Wissembourg, France) operating at 20 MHz for protons. The NMR probe temperature was controlled with a dedicated device (BVT 3000,

Bruker SA, Wissembourg, France) with temperature measurement accuracy of ± 0.15 °C. The instrument was equipped with a 10 mm probehead. Magnetic field tuning, homogeneity of the magnet, detection angles, receiver gain and pulse lengths were checked before each measurement. A pulse attenuation of 8 dB was used for measurements on the liquid phase.

Relaxometry. Different kinds of pulse sequences were used for NMR measurements, i.e. free induction decay (FID) and Carr–Purcell–Meiboom–Gill (CPMG) for relaxation time measurements. The CPMG were recorded with 10000 points and a spacing of 200 μ s between each echo. FIDs were measured for the determination of solid fat content and second moments. Twelve scans and a recycling delay (Rd) of 40 s were used for each measurement.

The CPMG signal was fitted by

$$s(t) = \sum_{i=1}^n A_i e^{-t/T_{2i}} \quad (1)$$

Solid fat content (SFC) and second moments M_2 were determined according to the model developed by Adam-Berret et al.²¹

$$s(t) = A e^{-(a^2 t^2)/2} \sin c(bt) + B e^{-t/c} \quad (2)$$

The second moment was determined by

$$M_2 = a^2 + \frac{1}{3} b^2 \quad (3)$$

SFC was estimated using the fitted parameters from eq 2: A corresponds to the total intensity of the solid signal, and B to the intensity of the liquid signal. SFC is thus determined by

$$\text{SFC} = \frac{A}{A + B} \times 100 \quad (4)$$

For eq 1, two fitting methods were used: the distributions of relaxation times were performed using the maximum entropy method (MEM) algorithm,³¹ and discrete values of T_2 were determined using the Levenberg–Marquardt algorithm (Table Curve 5.01). The fitting of eq 2 was only performed with the Levenberg–Marquardt algorithm.

Relaxation in Porous Media. In porous media, the spin–lattice relaxation time (T_1) and the spin–spin relaxation time (T_2) depend on the interactions with the surface of the pores. Due to the surface relaxation mechanism, the relaxation times are shorter in pores with a high surface-to-volume ratio. The relaxation parameters are therefore used to obtain information on pore geometry. The relationship between the relaxation times and the surface to volume can be expressed by^{28,29}

$$\frac{1}{T_{1/2}} = \frac{1}{T_{1/2\text{bulk}}} + \rho_{1/2} \frac{S}{V} \quad (5)$$

where $T_{1/2\text{bulk}}$ is the bulk relaxation time and $\rho_{1/2}$ is the surface relaxivity. S is the total surface accessible to the liquid phase, and V is the open pore volume.²⁶ In the fat crystal network, S corresponds to the specific surface area developed by the crystals, and V depends on the amount of liquid phase. The surface relaxivity is given by

$$\rho_{1/2} = \frac{\lambda}{T_{1/2\text{surface}}} \quad (6)$$

where λ is the thickness of molecular layer interacting with the surface of the pore. The relaxation times T_1 and T_2 on the surface are reduced by dipole–dipole interaction, cross relaxation or chemical exchange. The relaxivity is generally unknown, as is the case for triacylglycerols. The model presented above is exact only when the system is in the fast diffusive exchange limit, i.e. when molecules are mobile enough and the

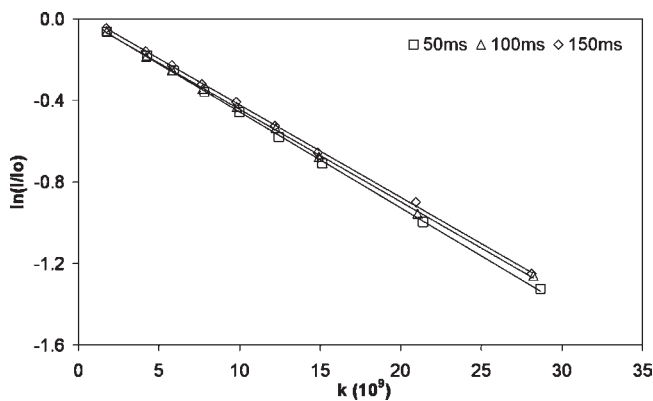


Figure 1. Evolution of $\ln(I/I_0)$ as a function of k as defined in eq 9 for 3 different diffusion times Δ .

exchange by diffusion between the molecule in the pore and the molecule at the surface is fast.

Diffusometry. For heterogeneous systems such as fluids in porous media, displacement of the diffusing species depends on the structure of the porous matrix and may be restricted by pore walls.^{25,32,33} Measuring the self-diffusion coefficients for different observation times can reveal information about pore size and pore connectivity (tortuosity). At very short diffusion times, molecules do not have the time to interact with the pore walls and the self-diffusion coefficient will equal the free diffusion coefficient of the fluid D_0 . When observation times increase, molecules can move in the whole pore and D_0 is influenced by the surface to pore volume ratio S/V . D levels off to an asymptotic value D_∞ reflecting the long-range connectivity of the porous medium, and the tortuosity can be derived from this measurement. The tortuosity τ which characterizes this connectivity is defined in eq 7:²⁸

$$\tau = \lim_{\Delta \rightarrow \infty} \frac{D_0}{D(\Delta)} \quad (7)$$

with D the diffusion time.

The self-diffusion coefficient of fluid molecules is determined by attenuation of the NMR spin echo signal as a function of an additionally applied external pulsed field gradient. The intensity of the NMR signal will decrease following eq 8:³⁴

$$S = S_0 \exp\left(-\gamma^2 \delta^2 g^2 D_0 \left(\Delta - \frac{\delta}{3}\right)\right) \quad (8)$$

where S is the signal intensity, S_0 is the signal intensity without gradients, γ is the gyromagnetic ratio ($= 2.68 \times 10^8 \text{ Hz} \cdot \text{T}^{-1}$ for ^1H), g is the intensity of the gradient, δ the duration of the pulse gradient and Δ is the duration between the two gradient pulses. K is defined as

$$K = -\gamma^2 g^2 \delta^2 \left(\Delta - \frac{\delta}{3}\right) \quad (9)$$

The decrease in signal intensity as a function of K for different Δ can be seen in Figure 1. The principle for the determination of D_0 was to vary g , the gradient intensity, and to fix the other parameters (Δ and δ). Figure 1 presents the variations of g for different Δ , the slope of the curve being D_0 .

PFG-NMR diffusion measurements were performed with a stimulated echo sequence (STE) for diffusometry for which 8 scans were acquired with a R_d of 3 s. Typical gradient parameters were $\delta = 0.7 \text{ ms}$ and g_{max} up to $2.5 \text{ T} \cdot \text{m}^{-1}$ with 8 different values of g . The diffusion times (Δ) varied in a range of 50 ms up to 250 ms, and the delay between the first and the second 90° pulses was 1 ms.

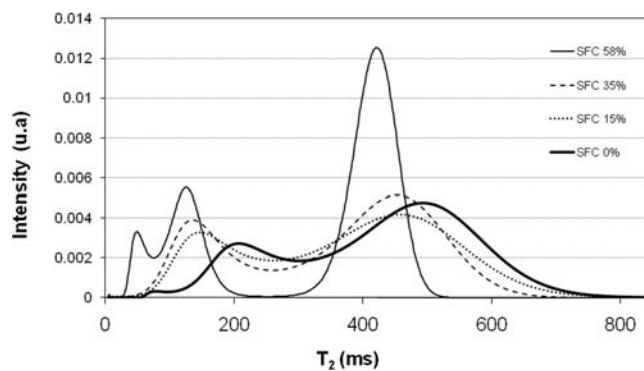


Figure 2. T_2 distribution of tricaprinn for different SFC value at 60°C .

RESULTS AND DISCUSSION

Effects of SFC on the Behavior of the Liquid Phase. Figure 2 summarizes the effects of SFC on the spin–spin relaxation times of tricaprinn in the liquid state for two weeks after crystallization.

For pure tricaprinn in the melt state a complex distribution from MEM with broad peaks was obtained for the relaxation times T_2 . This bimodal distribution may have different origins. The first assumption was that bimodal distribution is the result of inhomogeneous relaxation rates for the protons along the side chains. Indeed, it has been proved that the methyl group of fatty acids has a faster relaxation rate than the other carbons on the chain.^{23,24} This could provide wide distributions of relaxation times. However, the relaxation rates were determined on diluted triacylglycerols in a solvent and the mobility is probably different in a bulk system because of the liquid organization. The other possibility was linked to inhomogeneous organization of the triacylglycerols in the liquid with intermolecular interactions. Indeed, the liquid triacylglycerol organization is unknown and different types of organization could result in wide distributions.^{35,36}

For lower SFC, a bimodal distribution was obtained as for the pure tricaprinn in the melt, whereas a triexponential model was used to fit the CPMG signal for high SFC. The number of components used for the fitting from the Levenberg–Marquardt algorithm was provided by the relaxation time distributions determined by MEM. Two features should be pointed out: a change in the relative intensities of the relaxation time components and a decrease in the relaxation time values according to the SFC. The proportion of the component with a T_2 of 400 ms remained constant around 68% for all SFC, whereas the proportions of the other two relaxation components (T_2 around 50 ms and T_2 around 180 ms) evolved together. The intensity of the component with a T_2 around 180 ms increased whereas the intensity of the component with a T_2 around 50 ms decreased at the same time that SFC decreased (data not shown).

Two mechanisms can be assumed to explain the changes in T_2 value, an evolution of the composition of the liquid phase because of the presence of cocrystals, or interactions between the liquid and the fat crystal network as observed in porous media. Indeed, there were cocrystals in the liquid phase and thus a small amount of tristearin was dissolved in this phase.²⁰ There was an exchange between the solid and the liquid phase,³⁷ with recrystallization of tristearin on the surface which would decrease the viscosity and then would increase the T_2 . However, the exchange rate has been measured previously and was proved to be slow.^{37,38} This phenomenon was therefore not taken into account because of its only slight effects on the system during

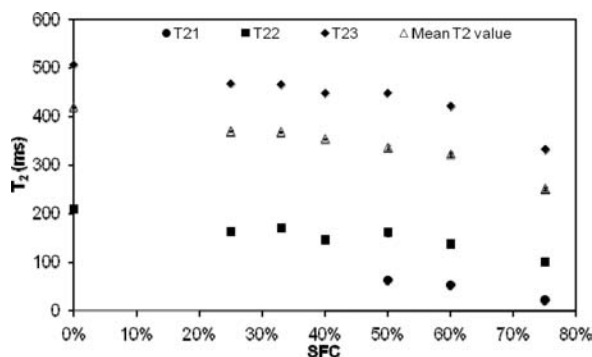


Figure 3. Evolution of the three components and the mean T_2 value as a function of SFC at 60 °C.

NMR measurements. The other possible mechanism is based on the relaxation mechanism in porous media with fast diffusive exchange between two fractions, a bulk fraction with a T_2 equal to that of the pure liquid phase and a surface fraction with a T_2 shortened by dipole interactions. The fast diffusive exchange limit is defined as³⁹

$$2\sqrt{2}\left(\frac{a^2}{\pi D}\right)\left(\frac{1}{T_{2s}} - \frac{1}{T_{2\text{bulk}}}\right) \ll 1 \quad (10)$$

If we considered a mean T_2 value for bulk, then $1/T_{2\text{bulk}}$ is equal to $1/0.420 = 2.38 \text{ s}^{-1}$ (Figure 3). For $1/T_{2s}$ we assumed that this value was in the range of the shortest T_2 measured for the largest SFC; then $1/T_{2s} = 1/0.020 = 50 \text{ s}^{-1}$. The self-diffusion coefficient for pure tricaprins was $0.086 \pm 0.008 \times 10^{-9} \text{ m}^2 \text{ s}^{-1}$. Therefore, the fast diffusive exchange limit is validated for pore size having a radius less than $1.42 \mu\text{m}$. The fat crystal network displays a structural hierarchy with individual fat crystals, crystal clusters and crystal network. The size of the crystal is in the micrometer range, and the size of the fat crystal clusters can vary from several micrometers to more than $200 \mu\text{m}$ according to the processing conditions and SFC.¹² If we assumed that the surface-to-volume ratio of the fat crystal involved in the clusters plays the main effect on the relaxation rate, then the condition for fast diffusive exchange limit is verified.

In previous results on porous media, the relaxation time of the liquid phase was described by a monoexponential decay.^{26,28} Since the relaxation time distributions of the pure liquid were broad, a mean relaxation time was determined from a weighted average of the values provided by the Levenberg–Marquardt algorithm. If we considered that the surface developed by the crystal at a long storage time is the same whatever the amount of fat crystal, then a linear relationship should be observed between $(1/T_{2\text{meas}} - 1/T_{2\text{bulk}})$ and the fat crystal volume estimated from the SFC according to eq 5. The evolution of $(1/T_{2\text{meas}} - 1/T_{2\text{bulk}})$ as a function of the ratio between the amount of solid phase and the amount of liquid phase at equilibrium is given in Figure 4. A linear relationship between $(1/T_{2\text{meas}} - 1/T_{2\text{bulk}})$ and the solid to liquid ratio was observed when the crystal network reached an equilibrium state after 12 days. According to the model presented in eq 5, the slope was proportional to the surface relaxivity and the surface of the crystals. According to eq 5, no constant should be added to the model. The constant identified from our experimental data could be due to the presence of tristearin in the liquid phase which affected the viscosity and then the T_2 , and also explained why the T_2 of the

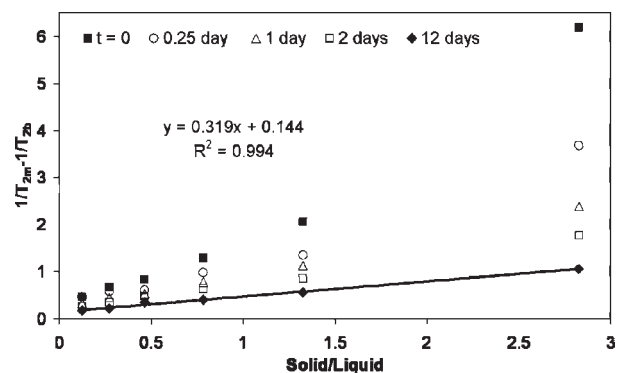


Figure 4. Evolution of $(1/T_{2\text{meas}} - 1/T_{2\text{bulk}})$ as a function of the solid to liquid ratio at different times at 60 °C.

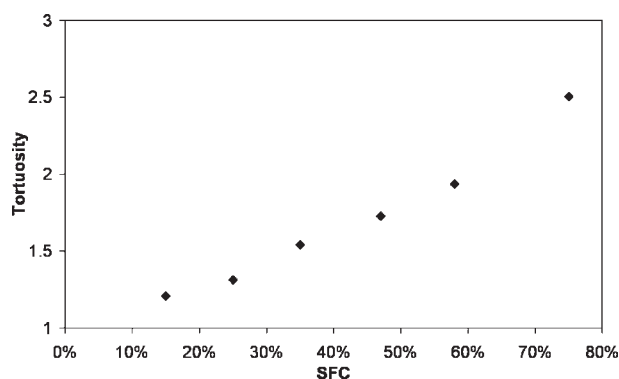


Figure 5. Evolution of tortuosity in the tricaprins–tristearin mixture as a function of SFC at 60 °C.

liquid tricaprins was not the same as the T_2 measured for the pure liquid tricaprins.

Figure 1 shows the evolution of the intensity of the PFG-NMR signal as a function of the gradient intensity for different Δ on the 50–50 blend. The attenuation was linear whatever the Δ , and no dependence of D on Δ was observed. This behavior was the same for all the mixtures (data not shown). When D is independent of Δ , it is possible to determine the tortuosity according to eq 7. For the determination of D_0 , the existence of the cocrystals which involved the presence of tristearin in the liquid phase was taken into account. A new D_0 was established by adding 3% (in weight) of tristearin dissolved in liquid tricaprins ($D_0 = 7.7 \times 10^{-11} \text{ m}^2 \cdot \text{s}^{-1}$). The tortuosity at 60 °C as a function of SFC is shown in Figure 5. The tortuosity decreased with decreasing SFC. It dropped from 2.3 for 75% SFC to 1.3 for 15% SFC. Such values are comparable to those found for polymers and silica.^{40,41}

Effects of Storage Time on NMR Parameters and Diffusion Coefficient of the Liquid Phase. The evolution of relaxation times over time was followed at 60 °C for different SFC. The SFC remained almost constant for the 2 weeks of measurements, and there was only a small decrease over time (data not shown). This decrease in SFC may have been related to the dissolution of tristearin in the liquid phase or attributable to the limitations of the Rd used during the measurements. Indeed, 12 accumulations were recorded for the SFC measurements with a Rd of 40 s, which was the maximum Rd for our apparatus. However, the T_1 of the crystalline phase was longer than 8 s and continued to increase over time.⁴ An error was thus generated in the intensity of the solid signal over accumulations because the solid phase had

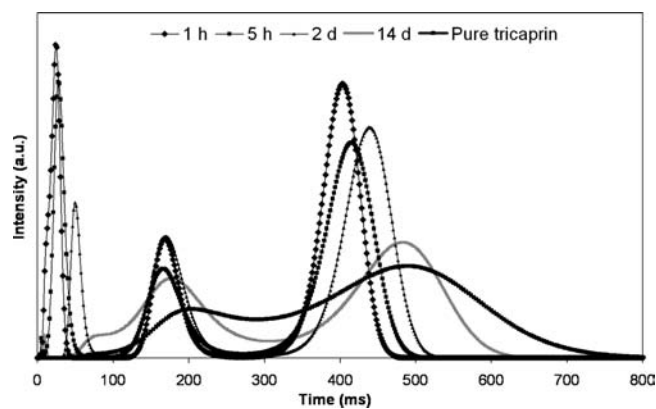


Figure 6. Evolution of the T_2 distributions of the 50–50 (w/w) tricaprinn–tristearin mixture over time at 60 °C.

not the time to relax completely between two accumulations. Consequently the SFC was underestimated, and as the T_1 continued to increase over time, the underestimation became greater, leading to a decrease in the SFC. At the same time, second moments (M_2) were determined in order to investigate any modifications of the polymorphism of the solid phase during the experiments. M_2 remained constant at around $1.05 \times 10^{10} \text{ s}^{-2}$. This value corresponded to the β polymorphic form of tristearin, and thus no polymorphic transformation of tristearin occurred over time.

The evolution of the distribution of the T_2 of the liquid phase was measured over time at 60 °C in order to follow the consequences of such crystal growth on the liquid phase (Figure 6). The 50–50 (w/w) mixture was chosen because of its intermediate behavior. It was first possible to see that the mixtures tended to the behavior of pure tricaprinn. Indeed, after 14 days, the distribution of the blend was close to the distribution of pure tricaprinn, with two broad peaks and a shoulder on the first peak, whereas the distributions were different after just 1 h. This meant that, after 14 days, tricaprinn in the mixture behaved as pure tricaprinn, and thus that the effect of the specific surface was weak and had little influence on the relaxation time. All the distributions were trimodal over time, but the peak intensity and the relaxation time values evolved differently according to the mixtures under consideration. During storage, the surface of the first peak decreased and the T_2 value associated with this peak increased from 26 to 75 ms. The surface of the second peak increased through broadening of the peak, and the peak remained centered on the same T_2 value around 170 ms. The third peak was similarly broadened over time, but the surface of the peak remained constant. The main effect on this peak was an increase in the T_2 value from 400 to 480 ms, almost the T_2 of pure tricaprinn (490 ms). The same evolution was observed for the other mixtures, except at 75% SFC where the relaxation time distribution after 14 days was still far from the distribution of pure tricaprinn (data not shown). The evolution of the T_2 values over time meant that the relaxation in the pore was different because of the modifications of the specific surface area developed by the crystals. In order to verify this hypothesis, a mean discrete value of T_2 was determined with the Levenberg–Marquardt algorithm for all the SFC and its evolution was followed over time (Figure 7). It was possible to see that there was a rapid increase during the first days and a slower increase subsequently. However the increase was more limited when the SFC was lower. The

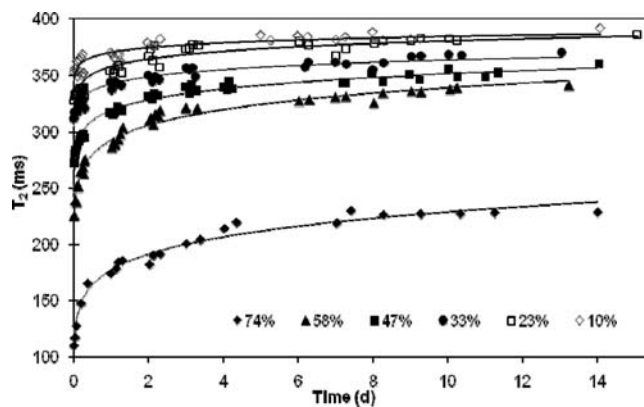


Figure 7. Evolution of mean T_2 of tricaprinn over time at different SFC.

Table 1. Parameters Obtained from the Power Law ($T_2 = cte t^K$) Fitting of the Mean T_2 of Tricaprinn over Time at Different SFC^a

SFC (%)	cte	K	R ²
75	177.1 ± 1.3	0.111 ± 0.004	0.98
57	292.4 ± 0.8	0.064 ± 0.002	0.98
48	318.9 ± 0.6	0.042 ± 0.001	0.98
35	342.5 ± 0.7	0.026 ± 0.001	0.94
25	357.6 ± 0.9	0.027 ± 0.001	0.91
15	370.3 ± 1.0	0.017 ± 0.001	0.8

^a See Figure 7.

T_2 of the liquid phase were fitted by a power law model as for the T_1 of the crystalline phase.⁴ Table 1 summarizes the parameters from the power law fitting for the different SFC. It has already been proved that the specific surface area of tristearin crystals in paraffin oil decreases over time,⁴² as does the average crystal size.⁴ This evolution in T_2 could thus be related to the decrease in the specific surface during storage, and the fact that the evolution according to a power law model was similar for the solid and the liquid phases confirmed this. Indeed, when crystals grew, the specific surface decreased and thus led to an increase in T_2 because the volume remained constant. The possibility that this increase could be due to the melting of cocrystals which would raise viscosity was considered. However, in this case, the T_2 would have been equal for all the SFC at equilibrium because the liquid phases would have the same composition, which was not the case.

Different behaviors were observed according to SFC. At 15% SFC, the T_2 rapidly reached the T_2 of pure tricaprinn, meaning that the effect of the surface on relaxation became negligible. It was thus not possible to study the evolution of the specific surface area subsequently. However, at 75% SFC the first values were low because of a large specific surface area which could be increased by the presence of many small crystals dispersed in the liquid phase and not participating in the network. These small crystals were melted by Ostwald ripening over time, leading to a decrease in the specific surface area.

In order to obtain information regarding tortuosity, the evolution of the diffusion coefficient at a long diffusion time, between 5 and 10 μm , was followed over time for the 6 different SFC at 60 °C (Figure 8). The diffusion coefficient remained constant over time for SFC > 23%, meaning that the tortuosity in

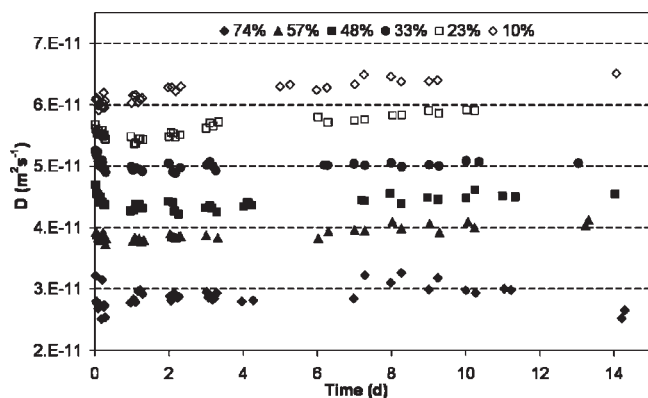


Figure 8. Evolution of diffusion coefficient of liquid tricaprinn over time for different SFC.

the fat crystal network was constant over time. The distance probed during diffusion measurements provided information on the average pore size, as the triacylglycerol molecules needed to probe at least this distance to report the effect of the surface on the diffusion coefficient. The pores investigated in this study were thus smaller than $5 \mu\text{m}$. It should be noted that there was a very small increase in diffusion coefficient over time for $\text{SFC} < 23\%$, which could be related to the decrease in tortuosity. Nevertheless, the dominating effect for diffusion in the fat crystal network remained the SFC, which increased the diffusion path. The combination of the measurements of the diffusion coefficient and T_2 relaxation time showed the evolution of the fat crystal network over time, since the specific surface area decreased but the tortuosity remained constant. The decrease in the specific surface area was thus due to melting of the small crystals. They would contribute to the thickness of the crystals, leading to a smaller surface. This hypothesis is supported by the X-ray diffraction and T_1 measurements previously performed on the same mixtures which proved an increase in the thickness of the crystals.⁴

Conclusion. The relaxation and the diffusion of the liquid phase in the fat crystal network were investigated. Two different effects were investigated: the SFC and storage time. The spin–spin relaxation time T_2 was proved to be sensitive to the effect of the specific surface area developed by the crystalline phase. There were two different changes in the specific surface area. First, the specific surface area was decreased over time by the melting of the small crystals because of Ostwald ripening. The small crystals recrystallized on the surface of the larger crystals, leading to an increase in the thickness of the crystals. This effect on the relaxation time of the liquid phase was greater when the SFC was higher, i.e. when there was less liquid and there were smaller crystals. Diffusion coefficient measurements provided information on the pore connectivity of the system. A linear relationship was observed between the tortuosity and the SFC. The fat crystal network was less tortuous at low SFC. However, the diffusion coefficient remained constant over time, meaning that the tortuosity did not change.

To conclude, NMR measurements can provide new parameters to characterize the microstructure of fat crystal networks.

AUTHOR INFORMATION

Corresponding Author

*F.M.: Cemagref, UR TERE, 17 Avenue de Cucillé, CS 64426, 35044 Rennes, France. Phone: (33) 2-23482178. Fax: (33) 2-23482115. E-mail: francois.mariette@cemagref.fr.

REFERENCES

- (1) Sato, K.; Ueno, S., Molecular interactions and phase behavior of polymorphic fats. In *Crystallization processes in fats and lipids systems*; Garti, N., Sato, K., Eds.; Marcel Dekker, Inc.: New York, 2001; pp 177–209.
- (2) Narine, S. S.; Marangoni, A. G. Relating structure of fat crystal networks to mechanical properties: a review. *Food Res. Int.* **1999**, *32* (4), 227–248.
- (3) Small, D. M. *The physical chemistry of lipids*, 1st ed.; Plenum Press: San Antonio, TX, 1986; Vol. 4, p 672.
- (4) Adam-Berret, M.; Riaublanc, A.; Rondeau-Mouro, C.; Mariette, F. Effects of crystal growth and polymorphism of triacylglycerols on NMR relaxation parameters. 1. Evidence of a relationship between crystal size and spin-lattice relaxation time. *Cryst. Growth Des.* **2009**, *9* (10), 4273–4280.
- (5) Walstra, P.; Kloek, W.; Van Vliet, T. Fat crystal networks. In *Crystallization processes in fats and lipid systems*; Garti, N., Sato, K., Eds.; Marcel Dekker, Inc.: New York, 2001; p 289.
- (6) Larsson, K. *Lipids-Molecular Organization, Physical Functions and Technical Applications*; The Oily Press: Dundee, 1994; Vol. 5, p 237.
- (7) Sato, K.; Ueno, S.; Yano, J. Molecular interactions and kinetic properties of fats. *Prog. Lipid Res.* **1999**, *38* (1), 91–116.
- (8) Cebula, D. J.; McClements, D. J.; Povey, M. J. W.; Smith, P. R. Neutron-Diffraction Studies of Liquid and Crystalline Trilaurin. *J. Am. Oil Chem. Soc.* **1992**, *69* (2), 130–136.
- (9) Corkery, R. W.; Rousseau, D.; Smith, P.; Pink, D. A.; Hanna, C. B. A case for discotic liquid crystals in molten triglycerides. *Langmuir* **2007**, *23* (13), 7241–7246.
- (10) Da Silva, E.; Rousseau, D. Molecular order and thermodynamics of the solid-liquid transition in triglycerides via Raman spectroscopy. *Phys. Chem. Chem. Phys.* **2008**, *10* (31), 4606–4613.
- (11) Sato, K. Crystallization behaviour of fats and lipids—a review. *Chem. Eng. Sci.* **2001**, *56* (7), 2255–2265.
- (12) Tang, D.; Marangoni, A. G. Microstructure and fractal analysis of fat crystal networks. *J. Am. Oil Chem. Soc.* **2006**, *83* (5), 377–388.
- (13) Van Den Tempel, M. Rheology of concentrated suspensions. *J. Colloid Interface Sci.* **1979**, *71* (1), 18–20.
- (14) Vreeker, R.; Hoekstra, L. L.; Denboer, D. C.; Agterof, W. G. M. The Fractal Nature of Fat Crystal Networks. *Colloids Surf.* **1992**, *65* (2–3), 185–189.
- (15) Tang, D.; Marangoni, A. G. Modified fractal model and rheological properties of colloidal networks. *J. Colloid Interface Sci.* **2008**, *318* (2), 202–209.
- (16) Liang, B.; Shi, Y.; Hartel, R. W. Correlation of rheological and microstructural properties in a model lipid system. *J. Am. Oil Chem. Soc.* **2008**, *85* (5), 397–404.
- (17) Norton, I. T.; Lee-Tuffnell, C. D.; Ablett, S.; Bociek, S. M. Calorimetric, NMR and X-RAY diffraction study of the melting behavior of tripalmitin and tristearin and their mixing behavior with triolein. *J. Am. Oil Chem. Soc.* **1985**, *62* (8), 1237–1244.
- (18) Van Duynhoven, J.; Dubourg, I.; Goudappel, G. J.; Roijers, E. Determination of MG and TG phase composition by time-domain NMR. *J. Am. Oil Chem. Soc.* **2002**, *79* (4), 383–388.
- (19) Trezza, E.; Haiduc, A. M.; Goudappel, G. J. W.; Van Duynhoven, J. P. M. Rapid phase-compositional assessment of lipid-based food products by time domain NMR. *Magn. Reson. Chem.* **2006**, *44* (11), 1023–1030.
- (20) Adam-Berret, M.; Riaublanc, A.; Mariette, F. Effects of crystal growth and polymorphism of triacylglycerols on NMR relaxation parameters. 2. Study of a tricaprinn-tristearin mixture. *Cryst. Growth Des.* **2009**, *9* (10), 4281–4288.
- (21) Adam-Berret, M.; Rondeau-Mouro, C.; Riaublanc, A.; Mariette, F. Study of triacylglycerol polymorphs by nuclear magnetic resonance: effects of temperature and chain length on relaxation parameters. *Magn. Reson. Chem.* **2008**, *46* (6), 550–7.
- (22) Gibon, V.; Blanpain, P.; Durant, F.; Deroanne, C. L. Application de la diffraction des rayons X, de la résonance magnétique nucléaire et de l'analyse calorimétrique différentielle à l'étude du polymorphisme

et de l'intersolubilité des triglycérides PPP, PSP et POP. *Belg. J. Food Chem. Biotechnol.* **1985**, *40* (5), 119–134.

(23) Le Botlan, D. J.; Helie, I. A Novel Approach to the Analysis of fats by low resolution NMR spectroscopy: application to milk and vegetable fats. *Analisis* **1994**, *22*, 108–113.

(24) Iwahashi, M.; Kasahara, Y.; Matsuzawa, H.; Yagi, K.; Nomura, K.; Terauchi, H.; Ozaki, Y.; Suzuki, M. Self-diffusion, dynamical molecular conformation, and liquid structures of n-saturated and unsaturated fatty acids. *J. Phys. Chem. B* **2000**, *104* (26), 6186–6194.

(25) Price, W. S.; Stilbs, P.; Soderman, O. Determination of pore space shape and size in porous systems using NMR diffusometry. Beyond the short gradient pulse approximation. *J. Magn. Reson.* **2003**, *160* (2), 139–143.

(26) Halperin, W. P.; Jehng, J. Y.; Song, Y. Q. Application of spin-spin relaxation to measurement of surface area and pore size distributions in hydrating cement paste. *Magn. Reson. Imaging* **1995**, *12*, 169–173.

(27) Hansen, E. W.; Fonnum, G.; Weng, E. Pore morphology of porous polymer particles probed by NMR relaxometry and NMR cryoporometry. *J. Phys. Chem. B* **2005**, *109* (51), 24295–24303.

(28) Latour, L. L.; Kleinberg, R. L.; Mitra, P. P.; Sotak, C. H. Pore-Size Distributions and Tortuosity in Heterogeneous Porous Media. *J. Magn. Reson.* **1995**, *112* (1), 83–91.

(29) Mitra, P. P.; Sen, P. N. Effects of microgeometry and surface relaxation on NMR pulsed-field-gradient experiments: Simple pore geometries. *Phys. Rev. B* **1992**, *45* (1), 143–156.

(30) Goudappel, G. J. W.; van Duynhoven, J. P. M.; Mooren, M. M. W. Measurement of oil droplet size distributions in food Oil/Water emulsions by time domain Pulsed Field Gradient NMR. *J. Colloid Interface Sci.* **2001**, *239*, 535–542.

(31) Mariette, F.; Guilleminot, J. P.; Tellier, C.; Marchal, P. Continuous Relaxation Time Distribution Decomposition by MEM. In *Signal Treatment and Signal Analysis in NMR*; Rutledge, D. N., Ed.; Elsevier: Paris, 1996; pp 218–234.

(32) Callaghan, P. T.; Coy, A.; Halpin, T. P. J.; Macgowan, D.; Packer, K. J.; Zelaya, F. O. Diffusion in porous systems and the influence of pore morphology in pulsed gradient spin-echo nuclear magnetic resonance studies. *J. Chem. Phys.* **1992**, *97*, 651–662.

(33) Hills, B. P.; Wright, K. M.; Snaar, J. E. M. Combined relaxation and diffusion studies of porous media using the multigrade CPMG sequence. *Magn. Reson. Imaging* **1996**, *14* (7–8), 715–718.

(34) Johnson, C. S. Diffusion ordered nuclear magnetic resonance spectroscopy: principles and applications. *Prog. Nucl. Magn. Reson. Spectrosc.* **1999**, *34* (3–4), 203–256.

(35) Callaghan, P. T. The use of ¹³C spin relaxation to investigate molecular motion in liquid tristearin. *Chem. Phys. Lipids* **1977**, *19* (1), 56–73.

(36) Callaghan, P. T.; Jolley, K. W. An irreversible liquid-liquid phase transition in tristerarin. *J. Chem. Phys.* **1977**, *67* (10), 4773–4774.

(37) Lofborg, N.; Smith, P.; Furo, I.; Bergenstahl, B. Molecular Exchange in Thermal Equilibrium between Dissolved and Crystalline Tripalmitin by NMR. *J. Am. Oil Chem. Soc.* **2003**, *80* (12), 1187–1192.

(38) Smith, K. W.; Smith, P. R.; Furo, I.; Pettersson, E. T.; Cain, F. W.; Favre, L.; Talbot, G. Slow recrystallization of tripalmitoylglycerol from MCT oil observed by ²H NMR. *J. Agric. Food Chem.* **2007**, *55* (21), 8585–8588.

(39) Belton, P. S.; Hills, B. P. The effects of diffusive exchange in heterogeneous systems on NMR pore shapes and relaxation processes. *Mol. Phys.* **1987**, *61* (4), 999–1018.

(40) Kuntz, J. F.; Palmas, P.; Level, V.; Canet, D. Restricted diffusion and exchange of water in porous media: Average structure determination and size distribution resolved from the effect of local field gradients on the proton NMR spectrum. *J. Magn. Reson.* **2008**, *191* (2), 239–247.

(41) Veith, S. R.; Hughes, E.; Vuataz, G.; Pratsinis, S. E. Restricted diffusion in silica particles measured by pulsed field gradient NMR. *J. Colloid Interface Sci.* **2004**, *274* (1), 216–228.

(42) Knoester, M.; De Bruyne, P.; Van Den Tempel, M. Crystallization of triglycerides at low supercooling. *J. Cryst. Growth* **1968**, *3–4*, 776–780.